



# Improved quantification of microbial CH<sub>4</sub> oxidation efficiency in arctic wetland soils using carbon isotope fractionation

I. Preuss, C. Knoblauch, J. Gebert, and E.-M. Pfeiffer

Institute of Soil Science, University of Hamburg, Hamburg, Germany

Correspondence to: I. Preuss (inken.preuss@uni-hamburg.de)

Received: 9 November 2012 – Published in Biogeosciences Discuss.: 4 December 2012

Revised: 12 March 2013 – Accepted: 18 March 2013 – Published: 16 April 2013

**Abstract.** Permafrost-affected tundra soils are significant sources of the climate-relevant trace gas methane (CH<sub>4</sub>). The observed accelerated warming of the arctic will cause deeper permafrost thawing, followed by increased carbon mineralization and CH<sub>4</sub> formation in water-saturated tundra soils, thus creating a positive feedback to climate change. Aerobic CH<sub>4</sub> oxidation is regarded as the key process reducing CH<sub>4</sub> emissions from wetlands, but quantification of turnover rates has remained difficult so far. The application of carbon stable isotope fractionation enables the in situ quantification of CH<sub>4</sub> oxidation efficiency in arctic wetland soils. The aim of the current study is to quantify CH<sub>4</sub> oxidation efficiency in permafrost-affected tundra soils in Russia's Lena River delta based on stable isotope signatures of CH<sub>4</sub>. Therefore, depth profiles of CH<sub>4</sub> concentrations and  $\delta^{13}\text{C}_{\text{CH}_4}$  signatures were measured and the fractionation factors for the processes of oxidation ( $\alpha_{\text{ox}}$ ) and diffusion ( $\alpha_{\text{diff}}$ ) were determined.

Most previous studies employing stable isotope fractionation for the quantification of CH<sub>4</sub> oxidation in soils of other habitats (such as landfill cover soils) have assumed a gas transport dominated by advection ( $\alpha_{\text{trans}} = 1$ ). In tundra soils, however, diffusion is the main gas transport mechanism and diffusive stable isotope fractionation should be considered alongside oxidative fractionation. For the first time, the stable isotope fractionation of CH<sub>4</sub> diffusion through water-saturated soils was determined with an  $\alpha_{\text{diff}} = 1.001 \pm 0.000$  ( $n = 3$ ). CH<sub>4</sub> stable isotope fractionation during diffusion through air-filled pores of the investigated polygonal tundra soils was  $\alpha_{\text{diff}} = 1.013 \pm 0.003$  ( $n = 18$ ). Furthermore, it was found that  $\alpha_{\text{ox}}$  differs widely between sites and horizons (mean  $\alpha_{\text{ox}} = 1.017 \pm 0.009$ ) and needs to be determined on a case by case basis. The impact of both fractionation factors on the quantification of CH<sub>4</sub> oxidation was analyzed by

considering both the potential diffusion rate under saturated and unsaturated conditions and potential oxidation rates. For a submerged, organic-rich soil, the data indicate a CH<sub>4</sub> oxidation efficiency of 50 % at the anaerobic–aerobic interface in the upper horizon. The improved in situ quantification of CH<sub>4</sub> oxidation in wetlands enables a better assessment of current and potential CH<sub>4</sub> sources and sinks in permafrost-affected ecosystems and their potential strengths in response to global warming.

## 1 Introduction

With a global warming potential 25 times as high as than carbon dioxide on a century time scale (Forster et al., 2007), methane (CH<sub>4</sub>) is an important greenhouse gas in the climate system. Much research effort focuses on identifying the global CH<sub>4</sub> sources and sinks to estimate not only their current strength but also their potential in response to land-use change and global warming (Walter et al., 2007; Dlugokencky et al., 2009; Keppler et al., 2006). In the focus of this study are arctic wetlands, which hold enormous amounts of organic carbon (Tarnocai et al., 2009; Zubrzycki et al., 2013) and are significant sources of CH<sub>4</sub> (Wille et al., 2008; Tagesson et al., 2012). With the observed accelerated warming of the Arctic, deeper permafrost thawing will cause increased carbon mineralization and CH<sub>4</sub> formation in water-saturated tundra soils, bearing the potential to cause positive feedback to climate change (Anisimov, 2007; Schuur et al., 2009; Åkerman and Johansson, 2008).

One of the key processes regulating wetland CH<sub>4</sub> fluxes is aerobic microbial CH<sub>4</sub> oxidation (Segers, 1998; Whalen, 2005) that is performed by methanotrophic bacteria.

CH<sub>4</sub> is formed in the final step of anaerobic microbial degradation of organic matter and is released from wetlands via three transport mechanisms: (1) diffusion along the concentration gradient between wetland soil and atmosphere, (2) ebullition in the form of gas bubbles due to CH<sub>4</sub> supersaturation, and (3) plant-mediated transport through gas conducting tissue known as aerenchyma (Joabsson et al., 1999; Lai, 2009; Whalen, 2005; Kutzbach et al., 2004). In contrast to the other two pathways, the slow diffusive flux facilitates extended contact of CH<sub>4</sub> with methanotrophic bacteria. This pathway may allow more than 90 % of the available CH<sub>4</sub> to be oxidized to CO<sub>2</sub> before it reaches the soil surface (Roslev and King, 1996; Sundh et al., 1995). The extent to which the CH<sub>4</sub> produced is oxidized, the CH<sub>4</sub> oxidation efficiency, is controlled by the key factors (1) rate of microbial oxidation (Wang et al., 2004) and (2) rate of diffusion of CH<sub>4</sub> (Curry, 2009; Dueñas et al., 1994). These parameters are mainly governed by the abundance and composition of methane oxidizing microbial communities and the environmental factors CH<sub>4</sub> and oxygen (O<sub>2</sub>) availability, soil air-filled porosity and soil-water content.

To quantify the CH<sub>4</sub> oxidation efficiency, several methods including batch or column laboratory experiments and in situ measurements are currently employed; yet, each displays different limitations (Huber-Humer et al., 2009). Gas push-pull tests (GPPT) inject and extract a defined volume of a gas mixture of a reactive gas (e.g., CH<sub>4</sub>) and a conservative tracer (e.g., argon) into and from the soil, and the microbial turnover is quantified by analyzing the breakthrough curves of the gases (Streese-Kleeberg et al., 2011). GPPTs are not easily applicable at sites with low oxidation rates and high water saturation (Gomez et al., 2008; Urmann et al., 2007), such as tundra wetlands, and have only been successfully applied in near-surface soils with a cylinder driven 50 cm into the soil (Nauer and Schroth, 2010). Furthermore, mass balance calculations using loading and surface flux measurements to determine the fraction of oxidized CH<sub>4</sub>, e.g., in biofilters or landfill cover soils (Powelson et al., 2007; Cabral et al., 2010; Gebert et al., 2003), are difficult to apply in wetlands since loading rates cannot be quantified in these open systems.

In addition to the above-mentioned methods, studies in landfill cover soils and swamp forests determined the CH<sub>4</sub> oxidation efficiency by measuring the changes in the ratio of two stable CH<sub>4</sub> isotopologues, <sup>13</sup>CH<sub>4</sub> and <sup>12</sup>CH<sub>4</sub> (Nozhevnikova et al., 2003; Chanton et al., 2008a; De Visscher et al., 1999, 2004; Happell et al., 1994; Liptay et al., 1998). The approach utilizes the fact that isotopic fractionation occurs when CH<sub>4</sub> is oxidized: the remaining CH<sub>4</sub> becomes heavier and the produced CO<sub>2</sub> becomes lighter (Barker and Fritz, 1981) as the light isotopologue <sup>12</sup>CH<sub>4</sub> is oxidized more readily by methanotrophic bacteria than the heavier <sup>13</sup>CH<sub>4</sub>. The isotopic fractionation factor  $\alpha$  is defined as the change in isotopic composition between reactant ( $Q$ )

and product ( $P$ ):

$$\alpha = \frac{R(^{13}\text{C}/^{12}\text{C})_Q}{R(^{13}\text{C}/^{12}\text{C})_P}, \quad (1)$$

where  $R$  is the isotope ratio of heavier <sup>13</sup>C and lighter <sup>12</sup>C. The enrichment of <sup>13</sup>C in CH<sub>4</sub> is measured as isotopic abundance relative to a standard, expressed in the  $\delta$  notation ( $\delta^{13}\text{C}$ ):

$$\delta^{13}\text{C} = \frac{R_{\text{sample}}}{R_{\text{standard}}} - 1, \quad (2)$$

where  $R_{\text{sample}}$  is the isotope ratio <sup>13</sup>C/<sup>12</sup>C of the sample and  $R_{\text{std}}$  is the <sup>13</sup>C/<sup>12</sup>C ratio of the reference standard VPDB (Vienna Peedee Belemnite;  $R_{\text{std}} = 0.0112372$ ) (McKinney et al., 1950).

Additionally to oxidation fractionation, Mahieu (2008) has shown through a model-based isotope approach that isotopic fractionation by diffusion should also be accounted for, given that the faster diffusive transport of the lighter isotope causes an enrichment of the heavier isotope in the remaining gas phase. In air, the diffusion coefficient of <sup>12</sup>CH<sub>4</sub> exceeds that of <sup>13</sup>CH<sub>4</sub> by a factor of 1.0195 due to mass differences. No fractionation is expected when advection dominates gas transport (Bergamaschi et al., 1998; Chanton, 2005).

For field applications the so-called “open-system equation” by Monson and Hayes (1980) is then applied to determine the CH<sub>4</sub> oxidation efficiency (Mahieu et al., 2008):

$$f_{\text{ox}} = \frac{(\delta_E - \delta_P)}{(\alpha_{\text{ox}} - \alpha_{\text{trans}})}, \quad (3)$$

where  $f_{\text{ox}}$  is the fraction of CH<sub>4</sub> oxidized in the soil;  $\delta_E$  is the  $\delta^{13}\text{C}$  of emitted CH<sub>4</sub> relative to VPDB;  $\delta_P$  is the  $\delta^{13}\text{C}$  of produced CH<sub>4</sub> relative to VPDB;  $\alpha_{\text{ox}}$  is the isotopic fractionation factor of oxidation;  $\alpha_{\text{trans}}$  is the isotopic fractionation factor of transport.

While for the microbial oxidation process isotopic fractionation factors ranging between 1.003 and 1.049 have been reported (Cabral et al., 2010; Templeton et al., 2006; Reeburgh et al., 1997), fractionation factors for gas transport are scarce and calculations of CH<sub>4</sub> oxidation efficiencies for landfill cover soils predominantly have assumed  $\alpha_{\text{trans}} = 1$ , supposing that gas transport of CH<sub>4</sub> is dominated by advection (Liptay et al., 1998). To our knowledge, the isotopic fractionation factor for diffusion has so far not been determined for soils, but only for a glass bead (diameter 2–3 mm) porous medium with  $\alpha_{\text{diff}} = 1.0178 \pm 0.001$  (De Visscher et al., 2004).

The objective of the current study is to improve a method for the quantification of microbial CH<sub>4</sub> oxidation efficiency in arctic wetlands based on the isotopic fractionation of CH<sub>4</sub> oxidation ( $\alpha_{\text{ox}}$ ) and gas transport ( $\alpha_{\text{trans}}$ ). The first measurement-based data of stable isotope fractionation during CH<sub>4</sub> diffusion ( $\alpha_{\text{diff}}$ ) through both water-saturated and

unsaturated wetland soils are presented. Furthermore, the impact of both isotopic fractionation factors on the quantification of CH<sub>4</sub> oxidation is estimated considering both the potential CH<sub>4</sub> diffusion rate at different soil-water contents and the potential CH<sub>4</sub> oxidation rates in the soil. CH<sub>4</sub> oxidation efficiency calculations are carried out with environmental data from a water-saturated tundra soil in Russia's Lena River delta, showing a CH<sub>4</sub> oxidation efficiency of up to 50 %.

## 2 Materials and methods

### 2.1 Study area

With its 32 000 km<sup>2</sup> the Lena River delta is the largest delta of the circum-arctic land masses. Situated at the north coast of Siberia, it belongs to the area of continuous permafrost with an arctic continental climate characterized by both low temperatures and precipitation (Boike et al., 2008). Investigations were carried out on Samoylov Island (72.22° N, 126.30° E) situated in the southern-central part of the delta. Samples were taken during two expeditions in 2009 and 2010 in the eastern part of the island that is characterized by wet polygonal tundra, a permafrost feature typical for extensive areas of arctic lowland tundra (French, 1996). Its microrelief consists of homogeneously spread soil units of depressed centers of low-centered ice wedge polygons (hereinafter *polygon center*) and their elevated surrounding rims. The soils only thaw in the upper part (< 60 cm) during the summer (active layer) and are rich in organic matter (Zubrzycki et al., 2013). According to the land cover classification of Schneider et al. (2009), the land cover class wet sedge- and moss-dominated tundra (WT) is the most important source of CH<sub>4</sub> in the Lena River delta. It consists of the subclasses dry sites (62.2 % cover), very wet sites (7.8 %), overgrown water (14.8 %) and water (15.2 %) (Schneider et al., 2009). This study investigated four polygon centers with differing water tables, thus representing all subclasses except the open water bodies: a polygonal pond with a permanent water level above the soil surface, two saturated polygon centers (A and B) with a changing water level close to the soil surface, and an unsaturated polygon center with a distinctly lower water level.

### 2.2 Soil sampling, storage and analysis

Soil samples were taken from every identified pedogenic horizon from the active layer of four polygon centers in pits which had been excavated to the frozen ground. Mixed soil samples were collected in plastic bags, refrozen in the field and kept frozen until arrival in the laboratory. In addition, three undisturbed soil cores (100 cm<sup>3</sup>, height 4 cm) were retrieved from each horizon, stored either cooled (samples 2009) or frozen (samples 2010) until further analysis.

Prior to analysis of the mixed organic samples, all living roots and plant material were removed. All mixed soil samples were air dried. The dried organic samples were cut into 2–5 mm pieces and the mineral samples were sieved (to < 2 mm). Subsequently, the samples were milled and dried at 105 °C. Total carbon and nitrogen were measured with an elemental analyzer (VarioMAX; Elementar, Hanau, Germany). Electrical conductivity (LF 90, WTW) and soil pH (CG 820, Schott) were determined in a suspension of 10 g of fresh soil in 50 mL of distilled water.

### 2.3 Vegetation analysis

Plant species were investigated according to the approach of Braun-Blanquet (1964) in three plots of 0.25 m<sup>2</sup> at each site. The species dominance of *Carex aquatilis* was estimated as the percentage of the basal area covering the plots.

### 2.4 Pore-water sampling, storage and gas concentration analyses

To measure profiles of CH<sub>4</sub> concentration and stable isotope (SI) ratio, pore-water samples were taken at several depths in the polygon center via perforated stainless steel tubes (∅ 3.18 mm), sampling 5 mL for concentration and 50 mL for SI analyses. Samples were conserved in vials or serum bottles flushed with nitrogen and containing sodium chloride, thus forming a saturated saline solution after injection. To liberate dissolved CO<sub>2</sub>, 100 µL of 10 % HCl solution was added afterwards.

Gas analyses were carried out at the field station on Samoylov Island and in the laboratory in Germany with gas chromatographs (both GC 7890, Agilent Technologies, Germany) equipped with a Poropak Q column (2 mm ID, 1.8 m length) separating CH<sub>4</sub> and CO<sub>2</sub>. CH<sub>4</sub> concentration was measured with a flame ionization detector (FID) and concentration of CO<sub>2</sub> with a thermal conductivity detector (TCD). Oven, injection, FID and TCD temperatures were 40, 75, 250 and 180 °C, respectively. Helium served as the carrier and make-up gas. The injection volume was 200 µL and samples were measured twice. Pore-water gas concentrations were calculated from the concentration measured and the headspace volume and pressure (pressure gauge LEO1, Fa. Keller, Switzerland) by applying Henry's Law and corrected for the partition of CH<sub>4</sub> between the aqueous and the gaseous phase by using the solubility coefficient  $\beta = 0.00867 \text{ mL mL}^{-1}$  for solubility of CH<sub>4</sub> in a saturated saline solution at 20 °C (Yamamoto et al., 1976; Kutzbach et al., 2004; Seibt et al., 2000). For calibration, CH<sub>4</sub> standard gases of 1.7 and 200 ppmv, 1, 10 and 50 vol. % were used. Uncertainty due to manual injection onto the column is < 1 % for the standards > 200 ppmv and < 18 % for the 1.7 ppmv standard.

Oxygen depth profiles were measured with a Fibox 3-trace v3 planar trace oxygen minisensor (Presens, Regensburg, Germany).

## 2.5 Isotope ratio mass spectrometry

Samples were analyzed in duplicate by gas chromatography isotope ratio mass spectrometry (GC-IRMS, Delta Plus, ThermoScientific, Dreieich, Germany) with a 25 m capillary column (Poraplot, 0.32 mm ID). Analytical replicate precision generally was < 0.2 ‰. For samples with near-atmospheric CH<sub>4</sub> concentrations, a preconcentration system (PreCon, ThermoScientific, Dreieich, Germany) was used (Brand, 1995) with standard error of replicate measurements generally less than 0.5 ‰. Injected sample volumes varied with sample concentrations (0.01–6 mL). Values are expressed relative to VPDB (Vienna Pee Dee Belemnite Standard) using the reference standard NGS3 8561 ( $\delta^{13}\text{C} = -73.27$  ‰ VPDB; NIST, Gaithersburg, USA).

## 2.6 Potential CH<sub>4</sub> oxidation rates

Potential CH<sub>4</sub> oxidation rates were determined for horizons of one saturated polygon center (saturated polygon center A) and the polygonal pond in batch cultures. Homogenized soil material (cut to < 2 mm, 4 g) with in situ water content was distributed in a thin layer over the side wall in flat-walled culture bottles (50 mL) to prevent substrate limitation effects. The flasks were closed with gas-tight butyl rubber stoppers through which CH<sub>4</sub> was added, giving an initial concentration of  $1.5 \pm 0.3$  ‰. Three flasks per sample were incubated horizontally in the dark at 4 °C for a few hours up to several weeks, depending on the oxidation rate.

CH<sub>4</sub> concentration in the headspace was measured over time by gas chromatography and oxidation rates were calculated from the declining CH<sub>4</sub> by linear regression analysis using 6–8 measurement points ( $R^2 > 0.81$ ,  $p < 0.01$ ).

## 2.7 Analysis of soil gas diffusivity

To analyze the effective diffusion coefficient for each soil horizon, the water content in the three undisturbed soil cores collected from each horizon of the polygon centers was adjusted to field capacity (0.3 kPa) on a sand bath. Afterwards, they were installed on top of cylindrical metal chambers of approximately 3 L volume, (Rolston, 1986). The chambers were filled with an initial CH<sub>4</sub> concentration of  $3.5 \pm 0.3$  mmol L<sup>-1</sup> (experiment runs > 10 h) and  $6.7 \pm 0.3$  mmol L<sup>-1</sup> (experiment runs > 10 h), which could only escape via diffusion through the soil core cylinders. Methanotrophic activity was blocked by addition of 0.8 mmol L<sup>-1</sup> acetylene. Diffusion was monitored by gas chromatography and rates were calculated via the decrease of CH<sub>4</sub> concentration inside the chamber over time. The inhibition of CH<sub>4</sub> oxidation by acetylene was verified by placing a soil core into a jar with an atmosphere of 3.5 mmol L<sup>-1</sup> CH<sub>4</sub>

and 0.8 mmol L<sup>-1</sup> acetylene. No CH<sub>4</sub> concentration change was detected over a period of three days.

To study the effect of pore-size distribution on diffusivity, samples of the unsaturated polygon center were consecutively drained in a pressure-plate apparatus (Richards and Fireman, 1943) using pressure heads of 6 kPa (drainage of macropores: > 50 μm Ø), 30 and 100 kPa (drainage of mesopores: 50–10 μm and ≤ 10 μm Ø), rerunning the experiment at each water content. Fick's first law was transformed to calculate the effective diffusion coefficient  $D_{\text{eff}}$  [m<sup>2</sup> s<sup>-1</sup>] as follows:

$$D_{\text{eff}} = -J_{\text{CH}_4} \left( \frac{dc}{dx} \right)^{-1}, \quad (4)$$

where  $J_{\text{CH}_4}$  is the diffusive CH<sub>4</sub> flux (mol m<sup>-2</sup> s<sup>-1</sup>),  $dx$  is the distance of which diffusion occurs through, i.e., height of cylinder (m), and  $dc$  is the concentration difference between chamber and atmosphere (mol m<sup>-3</sup>).

The final value of  $D_{\text{eff}}$  for each soil core was calculated as an average of six individual measurements. Experiments were either carried out at room temperature or, when run for more than one day, in an incubator at 20 °C and 98–100 % relative humidity to minimize evaporation effects. Molar concentrations were corrected for temperature and pressure according to the ideal gas law. Soil cores were weighed at each dewatering stage to determine the water content and air-filled porosity. The chambers were tested for leaks with the first experimental setup using a resin casted core.

The experimental setup was modified with a second chamber to determine the diffusion through water-saturated soils. First, the diffusion chamber was filled with distilled water adjusted to pH 2 with phosphoric acid and initially contained 1.44 mmol L<sup>-1</sup> CH<sub>4</sub> and 0.8 mmol L<sup>-1</sup> acetylene. Three water-saturated soil cores of the uppermost horizon of the saturated polygon center B were installed on top of the chamber. Then a second chamber (1.4 L volume) was installed on top of the cylinder containing the undisturbed soil sample. The top chamber was subsequently filled with distilled water at pH 2. With this experimental setup, CH<sub>4</sub> diffusion from the bottom chamber through the water-saturated soil sample into the top chamber could be measured. Within 4 h the solution of the bottom chamber was sampled 3–4 times by collecting 3 mL water with a syringe and a hypodermic needle through a rubber stopper at one side of the chamber and simultaneously injecting 3 mL of the initial solution at the other side of the chamber. Samples were conserved in vials flushed with nitrogen and containing sodium chloride. Experiments were run consecutively and at 20 °C to minimize expansion effects of the solutions. Gas diffusivity was calculated from the decreasing gas concentration in the bottom chamber.

To prevent CH<sub>4</sub> production in the water-saturated soil samples during diffusion measurements, the undisturbed soil samples were set into a solution of 10 mmol L<sup>-1</sup>

2-bromoethane-sulfonate (an inhibitor of methanogenesis) dissolved in distilled water for more than five days prior to the experiment. The inhibition of methanogenesis and CH<sub>4</sub> oxidation in the second experimental setup was verified by placing the treated soil cores into jars with distilled water adjusted to pH 2 and 1.44 mmol L<sup>-1</sup> CH<sub>4</sub> and 0.8 mmol L<sup>-1</sup> acetylene. Neither a decrease nor increase of CH<sub>4</sub> was detected.

After the diffusion experiments, core samples were dried to a constant weight at 105 °C and the total porosity was determined by helium pycnometry (AccuPyc II 1340, Micromeritics, Norcross, USA). The volumetric water content was subtracted from the total porosity to obtain the air-filled porosity.

## 2.8 Determination of $\alpha_{\text{ox}}$ and $\alpha_{\text{diff}}$

To determine the fractionation factors for oxidation and diffusion, gas samples from the batch oxidation experiment measurements and gas or water samples from the diffusion chambers were analyzed for  $\delta^{13}\text{C}_{\text{CH}_4}$  composition.

Both experimental setups are closed systems where a limited supply of reactant, CH<sub>4</sub>, undergoes an irreversible conversion to a product, CO<sub>2</sub>, which is either constantly removed (in the diffusion experiment) or remains in the system (in the batch experiment) without further reacting with the reactant. In this respect, closed system kinetic fractionation behaves like open system fractionation, where CH<sub>4</sub> is constantly removed. Assuming Rayleigh (1896) open system fractionation, the isotopic fractionation factor was calculated based on the approach described in Coleman et al. (1981):

$$\delta^{13}\text{C}_t \cong (((1/\alpha) - 1) \times \ln(M_t/M_0)) + \delta^{13}\text{C}_0, \quad (5)$$

where  $M_0$  is the concentration of CH<sub>4</sub> at time 0,  $M_t$  is the concentration of CH<sub>4</sub> at time  $t$ ,  $\delta^{13}\text{C}_0$  is the  $\delta^{13}\text{C}$  value of CH<sub>4</sub> at time 0, and  $\delta^{13}\text{C}_t$  is the  $\delta^{13}\text{C}$  value of CH<sub>4</sub> at time  $t$ . From the slope ( $m$ ) of the linear regression between the differences in CH<sub>4</sub> isotope values ( $\delta^{13}\text{C}_t - \delta^{13}\text{C}_0$ ) and the fraction of the remaining CH<sub>4</sub> concentration ( $\ln(M_t/M_0)$ ) the isotopic fractionation factor can be derived as follows:

$$\alpha = \frac{1}{(m+1)}. \quad (6)$$

Fractionation factors were determined for three replicates each with at least five gas samples. The fractionation factor for diffusion at water saturation was determined for three replicates with 3–4 water samples each.

## 2.9 CH<sub>4</sub> oxidation efficiency calculations

The isotopic fractionation factors  $\alpha_{\text{ox}}$  and  $\alpha_{\text{diff}}$  were then used to calculate the CH<sub>4</sub> oxidation efficiency from the  $\delta^{13}\text{C}_{\text{CH}_4}$  isotopic signatures at different soil depths of the saturated polygon center A sampled on 19 July 2009. Calculations were made for horizons where both a decrease in concentration and an enrichment of <sup>13</sup>C in CH<sub>4</sub> were observed

and diffusion was assumed to be the main occurring transport mechanism ( $\alpha_{\text{trans}} = \alpha_{\text{diff}}$ ) using Eq. (3). Comparatively, to determine the CH<sub>4</sub> oxidation efficiency under the assumption that no fractionation by transport occurs, the calculations were repeated with  $\alpha_{\text{trans}} = 1$ . In addition, calculations were conducted with the mean, minimum and maximum of both fractionation factors of all investigated sites to estimate their impact on  $f_{\text{ox}}$ .

To account for a potential impact of temperature on the isotopic fractionation during CH<sub>4</sub> oxidation, calculations were additionally conducted with a temperature-dependent correction for  $\alpha_{\text{ox}}$ , decreasing with rising temperature by  $3.9 \times 10^{-4} \text{ °C}^{-1}$  (Chanton et al., 2008b).

## 2.10 Statistical analyses

Statistical analyses were performed using OriginPro 8G (OriginLab Corporation, USA). The relationship between air-filled porosity and soil gas diffusion was curve fitted and examined with a one-way ANOVA. Correlations between oxidation rate and  $\alpha_{\text{ox}}$  and between diffusion coefficients and  $\alpha_{\text{diff}}$  were tested with Pearson's correlation analysis. Isotopic fractionation factors of different sites were compared with one-way ANOVAs and a post-hoc Tukey's honestly significant differences test (Tukey's).

## 3 Results

### 3.1 Soil and vegetation characteristics

In the depressed polygon centers, drainage was impeded by the underlying permafrost. Thus, the soils of the polygon centers were mostly water saturated with a varying water level close to the surface. All polygon centers were characterized by reducing conditions facilitating anaerobic degradation of organic matter. The two saturated polygon centers and the unsaturated polygon center showed a very high organic carbon content in the upper horizons (> 120 mg g<sup>-1</sup> OC, designated as Oi according to US Soil Taxonomy (2010), Table 1). Subjacent horizons (A, Oi) showed an accumulation of humified organic matter mixed with fine sand bands and hydromorphic features (Bg). According to the US Soil Taxonomy, the soils of these three polygon centers were classified as *Typic Aquorthel* (USDA, 2010), and as *Histic Crysol* according to the World Reference Base (WRB, 2006).

The saturated polygonal pond was characterized by a more uniform accumulation of organic carbon across the profile (ranging around 60 mg g<sup>-1</sup> OC), containing fine sand and showing features of gleying. The soil of this polygon center was classified as *Typic Aquorthel* (USDA, 2010), and *Typic Crysol* (WRB, 2006).

The total porosity of the upper horizons ranged around 90%, decreasing within the profile to 50%. Accordingly, air-filled porosity at field capacity was high in the top horizons (> 18%) and the bulk density was low

**Table 1.** Selected physical soil properties. Horizon designation according to US Soil Taxonomy (USDA, 2010).

Site	Horizon	Depth below soil surface (cm)	pH	Electrical conductivity (μS)	Total porosity (%)	Air-filled porosity at field capacity (%)	Water content at field capacity (vol %)	Bulk density (g cm <sup>-3</sup> )	OC (mg g <sup>-1</sup> )	Soil texture & further characteristics
Saturated polygon center A	Oi	0–5	5.6	90.7	90.2 ± 0.6	22.2 ± 2.8	68.0 ± 2.4	0.22 ± 0.01	177	Slightly decomposed plant material, <i>Carex</i> rhizomes
	AOi	5–10	5.5	37.8	91.6 ± 0.6	27.7 ± 6.1	63.9 ± 5.5	0.19 ± 0.01	108	Slightly humified plant material, <i>Carex</i> rhizomes, pure fine sand
	A1	10–18	5.5	49.4	69.0 ± 1.8	3.8*	65.7 ± 0.9	0.79 ± 0.05	30	Humified organic matter, slightly silty fine sand
	A2	18–33	5.6	48.7	80.8 ± 1.7	1.8 ± 1.3**	79.9 ± 1.7	0.46 ± 0.04	42	Humified organic matter, fine sand bands, frozen ground below
Saturated polygon center B	Oi	0–5	6.0	83.8	88.24**	n.a.	n.a.	0.27**	202	Slightly decomposed plant material, <i>Carex</i> rhizomes
Unsaturated polygon center	Oi1	0–3	5.6	153.9	93.4 ± 2.4	32.8 ± 10.2	60.6 ± 8.0	0.15 ± 0.05	125	Slightly decomposed plant material, <i>Carex</i> rhizomes
	Oi2	3–12	5.6	73.3	94.9*	18.32*	72.0 ± 6.8	0.10 ± 0.00	150	Slightly decomposed plant material, <i>Carex</i> rhizomes
	A	12–22	5.6	40.8	92.3 ± 0.4	32.0 ± 2.6	60.3 ± 2.4	0.16 ± 0.01	87	Humified organic matter, slightly silty fine sand
	Bg	22–28	5.9	34.8	54.4 ± 2.9	1.7*	56.0 ± 0.3	1.19 ± 0.08	15	Medium silty fine sand, frozen ground below
Polygonal pond	A	0–7	5.4	30.6	89.7 ± 0.6	33.2 ± 7.4	56.4 ± 6.8	0.23 ± 0.01	60	Slightly decomposed plant material, containing fine sand bands
	Ag1	7–17	5.4	28.6	85.8 ± 1.5	22.0 ± 3.6	63.8 ± 2.2	0.34 ± 0.04	65	Humified organic matter, fine sand bands, gleying
	Ag2	17–29	6.0	24.2	77.1 ± 1.2	6.8 ± 1.1	70.3 ± 2.3	0.57 ± 0.04	60	Humified organic matter, fine sand bands, gleying
	ABg (2010)	17–43	6.1	86.2	65.4 ± 1.8	5.8 ± 1.3	59.5 ± 2.4	0.88 ± 0.05	54	Humified organic matter, slightly silty fine sand bands, gleying, frozen ground below

\*\* One replicate only, \* two replicates only, n.a. = not analyzed.

(< 0.3 g cm<sup>-3</sup>) in comparison to the more mineral horizons above the frozen ground.

The vegetation of all polygon centers was dominated by the hydrophilic sedge *Carex aquatilis*, covering 25 ± 3 % of the basal area of the saturated polygon center A, 17 ± 4 % of the saturated polygon center B, 27 ± 10 % of the unsaturated polygon center and 6 ± 1 % of the polygonal pond. The unsaturated polygon center was further covered by the mosses *Limprichtia revolvens* and *Meesia longiseta* and the polygonal pond by the submerged brown moss *Scorpidium scorpioides*.

### 3.2 Potential CH<sub>4</sub> oxidation rates and isotopic fractionation associated with oxidation

High potential CH<sub>4</sub> oxidation rates occurred in samples from the two organic-rich top horizons of the saturated polygon center (Oi: 31.7 ± 2.3 nmol h<sup>-1</sup> g dw<sup>-1</sup>; AOi: 18.8 ± 8.4 nmol h<sup>-1</sup> g dw<sup>-1</sup>, Table 2). In comparison, the upper horizons of the polygonal pond featured lower potential CH<sub>4</sub> oxidation rates (A: 4.4 ± 0.3 nmol h<sup>-1</sup> g dw<sup>-1</sup>; Ag1: 6.1 ± 4.4 nmol h<sup>-1</sup> g dw<sup>-1</sup>). The lowest horizon of the polygonal pond showed a high potential CH<sub>4</sub> oxidation rate of 49.2 ± 7.7 nmol h<sup>-1</sup> g dw<sup>-1</sup>.

The isotopic fractionation during oxidation was highest in the top horizons of the saturated polygon center (Oi: α<sub>ox</sub> = 1.031 ± 0.002, Table 2). Low isotopic fractionation was detected for the two upper soil horizons of the polygonal pond (A: α<sub>ox</sub> = 1.005 ± 0.001; Ag1: α<sub>ox</sub> = 1.009 ± 0.007), corresponding with low oxidation activities found in this experimental setup. In comparison, the calculated isotopic fractionation factors of the lower horizons were higher (Ag2: α<sub>ox</sub> = 1.017 ± 0.001; ABg: α<sub>ox</sub> = 1.020 ± 0.002). There was a significant positive correlation between oxidation rates and α<sub>ox</sub> (Pearson's correlation coefficient  $r = 0.6$ ;  $p < 0.01$ ,  $n = 18$ ). Furthermore, isotopic fractionation factors associated with oxidation differed significantly between sites (ANOVA, Tukey's,  $p < 0.01$ ,  $n = 18$ ).

### 3.3 Analysis of soil gas diffusivity and isotopic fractionation associated with diffusion

Under water-saturated conditions the potential CH<sub>4</sub> diffusion rates were low with 0.5 ± 0.3 nmol h<sup>-1</sup> m<sup>-2</sup> ( $n = 3$ ; Table 2). At field capacity, the polygonal pond was characterized by higher potential diffusion rates than the saturated polygon center, with the highest rate found in the upper horizon (39.6 ± 26.9 nmol h<sup>-1</sup> m<sup>-2</sup>). Potential diffusion rates decreased from upper to lower horizons with the exception of a

**Table 2.** Potential methanotrophic activity, potential rates of CH<sub>4</sub> diffusion and isotopic fractionation factors for diffusion and oxidation calculated for the different horizons of the studied sites. Potential diffusion rates of the saturated polygon center A and the polygonal pond were determined at field capacity (0.3 kPa) and of the saturated polygon center B at water saturation; n.a. = not analyzed.

Water potential	Site	Horizon	Mean depth below soil surface, cm	Potential CH <sub>4</sub> oxidation rate, nmol h <sup>-1</sup> g dw <sup>-1</sup> (mean ± SD)	α <sub>ox</sub> (mean ± SD)	Potential CH <sub>4</sub> diffusion rate, nmol h <sup>-1</sup> m <sup>-2</sup> (mean ± SD)	α <sub>diff</sub> (mean ± SD)
Water saturated	Saturated polygon center B	Oi	2.5	n.a.	n.a.	0.5 ± 0.3	1.001 ± 0.000
		Saturated polygon center A	Oi	2.5	31.7 ± 2.3	1.031 ± 0.002	9.8 ± 6.2
0.3 kPa	Saturated polygon center A	AOi	7.5	18.8 ± 8.4	1.023 ± 0.002	8.8 ± 4.2	1.014 ± 0.001
		Polygonal pond	A	3.5	4.4 ± 0.3	1.005 ± 0.001	39.6 ± 26.9
		Ag1	12.5	6.1 ± 4.4	1.009 ± 0.007	17.0 ± 11.3	1.013 ± 0.002
		Ag2	25	7.3 ± 1.8	1.017 ± 0.001	2.9 ± 0.7	1.011 ± 0.000
		ABg (2010)	33	49.2 ± 7.7	1.020 ± 0.002	9.6 ± 1.5	1.017 ± 0.001

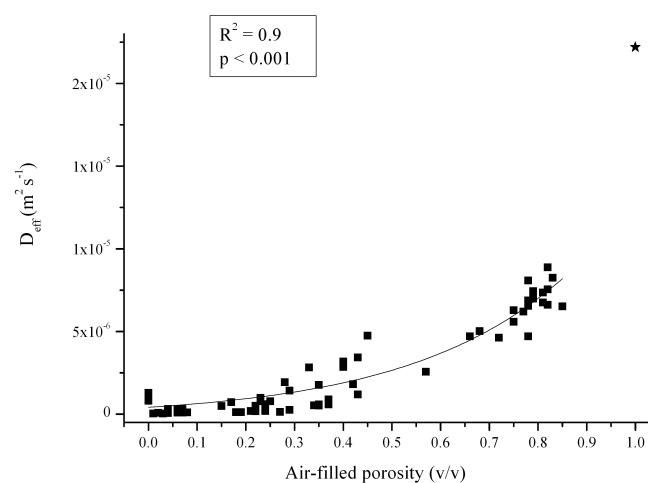


**Fig. 1.** Relationship between air-filled porosity and soil gas diffusion (effective diffusion coefficient) with exponential fit,  $n = 64$ . Star marks diffusion coefficient of CH<sub>4</sub> ( $D = 2.2 \times 10^{-5} \text{ m}^2 \text{ s}^{-1}$ ) in free air at 20 °C and 101.33 kPa given by Coward and Georgeson (1937).

mid-range rate ( $9.6 \pm 1.5 \text{ nmol h}^{-1} \text{ m}^{-2}$ ) in the lowest horizon of the polygonal pond.

Diffusion tests under different water contents showed that diffusion predominantly took place through macropores in each horizon of both sites (see Table 3). Once the macropores were drained (6 kPa), the diffusion was faster than at field capacity, but did not change strongly during further drainage. The lowest horizon was characterized by the lowest diffusion coefficient in each case. Diffusivity measurements at different water contents showed that the diffusion coefficient exponentially increased with an increasing volume of air-filled pore space ( $R^2 = 0.9$ ,  $p < 0.001$ ,  $n = 64$ ,  $D_{\text{eff}} = -8.27237 \times 10^{-7} + 8.89081 \times 10^{-7} \times e^{(2.71241 \times \Phi a)}$  where  $\Phi a$  is the air-filled pore space, Fig. 1).

Isotopic fractionation by diffusion under unsaturated conditions ranged between 1.007 and 1.018 (Table 2). Values for  $\alpha_{\text{diff}}$  did not correlate significantly with diffusion coefficients (Pearson's correlation coefficient  $r = -0.1$ ;  $p > 0.05$ ,  $n = 18$ ) and did not differ significantly between sites (ANOVA, Tukey's,  $p > 0.05$ ,  $n = 18$ ), with a mean  $\alpha_{\text{diff}} = 1.013 \pm 0.003$ . Almost no isotopic fractionation by diffusion was detected under water-saturated conditions with  $\alpha_{\text{diff}} = 1.001 \pm 0.000$  ( $n = 3$ ).

### 3.4 CH<sub>4</sub> oxidation efficiency calculations

To investigate the potential impacts of the measured isotopic fractionation factors on the oxidation efficiency estimates, the CH<sub>4</sub> oxidation efficiency was calculated based on the stable carbon isotope signatures of CH<sub>4</sub> sampled in the soil-water phase of the saturated polygon center A on 19 July 2009 (see Fig. 2). During sampling, the *Typic Aquorthel* featured a water level 9 cm above soil surface and a thawing depth of 30 cm.

The highest CH<sub>4</sub> concentration was found close to the frozen ground and decreased from there to 9 cm by 88 %. A CH<sub>4</sub> concentration peak at 6.5 cm was followed by a further decrease to near-atmospheric concentrations towards the water surface (4 cm above soil surface in the pond water). Concurrently, the  $\delta^{13}\text{C}$  values of CH<sub>4</sub> fluctuated between the frozen ground and 9 cm within 2.5 ‰ ( $-56.8 \pm 1.1$  ‰), decreasing between 6.5 and 1.5 cm from  $-53.8$  ‰ to  $-58.3$  ‰ and then increasing towards the water surface ( $-44.9$  ‰). Two O<sub>2</sub> profile measurements during the same month (Fig. 2) showed that O<sub>2</sub> was depleted ( $< 3 \mu\text{mol L}^{-1}$ ) within the first horizon (Oi); thus, the main part of oxidation presumably only occurred close to the soil surface.

Employing the isotopic fractionation factors (Oi  $\alpha_{\text{ox}} = 1.031$ ;  $\alpha_{\text{trans}} = \alpha_{\text{diff}} = 1.001$  for water-saturated conditions) a CH<sub>4</sub> oxidation efficiency of  $f_{\text{ox}} = 45$  % was assessed between 1.5 and  $-4$  cm by assuming diffusion

**Table 3.** CH<sub>4</sub> diffusion coefficients of an unsaturated polygon center at the different dewatering levels 0.3, 6, 30 and 100 kPa at different soil depths (mean ± std, *n* = 3).

Site	Horizon	Mean depth below soil surface in cm	Diffusion coefficients in $10^{-6} \times \text{m}^2 \text{s}^{-1}$ (mean ± SD) at dewatering levels of			
			0.3 kPa	6 kPa	30 kPa	100 kPa
Unsaturated polygon center	Oi1	1.5	0.70 ± 0.47	5.52 ± 2.29	6.72 ± 2.14	7.15 ± 2.08
	Oi2	8	0.40 ± 0.16	5.22 ± 1.02	7.15 ± 1.03	7.48 ± 1.30
	A	17.5	0.67 ± 0.21	4.98 ± 0.69	6.37 ± 0.85	6.80 ± 1.11
	Bg	26.5	0.24 ± 0.17	0.75 ± 0.33	2.18 ± 0.77	3.15 ± 0.99

**Table 4.** Calculated CH<sub>4</sub> oxidation efficiency  $f_{\text{ox}}$  in percent for the saturated polygon center A (“saturated pc”) between 1.5 cm below ( $\delta_P$ ) and 4 cm above ( $\delta_E$ ) soil surface according to Eq. (3) applying the fractionation factors  $\alpha_{\text{ox}}$  and  $\alpha_{\text{diff}}$  of the respective horizon (horizon Oi). Calculations were further conducted with the mean, minimum and maximum of both fractionation factors of all investigated sites, with  $\alpha_{\text{ox}}$  corrected for temperature according to Chanton et al. (2008b) and with  $\alpha_{\text{trans}} = 1$  (no fractionation due to transport).

Saturated polygon center A			$\alpha_{\text{trans}}$					
$\delta_E$	–4 cm:	–44.9‰	no fractionation	$\alpha_{\text{diff}}$				
				saturated pc Oi		all sites		
$\delta_P$	1.5 cm:	–58.3‰	1.000	water saturated	field capacity	mean	min.	max.
								1.001
$\alpha_{\text{ox}}$	mean	1.017	79	84	447	335	134	–1340
	all sites min.	1.004	335	447	–134	–149	–447	–96
	max.	1.032	42	43	74	71	54	96
	saturated pc Oi	1.031	43	45	79	74	56	103
	temp corr.	1.028	48	50	96	89	64	134

to be the sole transport mechanism (see Table 4). These values of CH<sub>4</sub> oxidation efficiency approximated those assuming that no CH<sub>4</sub> isotope fractionation associated with transport mechanisms took place  $\alpha_{\text{trans}} = 1$ , e.g., in case that ebullition or plant-mediated transport dominate. The fraction of oxidized CH<sub>4</sub> ( $f_{\text{ox}}$ ) in this case would account for 43 % of the produced CH<sub>4</sub>.

Assuming unsaturated conditions with a water content at field capacity ( $\alpha_{\text{trans}} = \alpha_{\text{diff}} 0.3 \text{ kPa} = 1.014$ ), the same  $\delta^{13}\text{C}$  profile would result in a CH<sub>4</sub> oxidation efficiency almost twice as high as under water-saturated conditions ( $f_{\text{ox}} = 79\%$  between 1.5 and –4 cm; Table 4) when using the determined  $\alpha_{\text{ox}}$  of 1.031. Calculations with the mean, maximum and minimum of both fractionation factors of all sites measured under unsaturated conditions showed highly varying results (Table 4). Moreover, the CH<sub>4</sub> oxidation efficiency estimates negative values when  $\alpha_{\text{diff}} > \alpha_{\text{ox}}$ . However, calculations using  $\alpha_{\text{ox}}$  of the saturated polygon center and the mean  $\alpha_{\text{diff}}$  of all sites showed results close to the calculations using  $\alpha_{\text{diff}}$  at field capacity of the saturated polygon center with  $f_{\text{ox}} = 74\%$  (Table 4).

While  $\alpha_{\text{ox}}$  was determined in the experiments at 4 °C, in situ temperature profiles indicated higher temperatures in the

significant soil horizon on 19 July 2009 (1.5 cm: 12.4 °C). Applying the temperature-dependent correction by Chanton et al. (2008b), the corrected isotopic fractionation factor of Oi was  $\alpha_{\text{ox}} = 1.028$ , resulting in a CH<sub>4</sub> oxidation efficiency of  $f_{\text{ox}} = 50\%$  in the topmost horizon (Table 4).

## 4 Discussion

### 4.1 Potential CH<sub>4</sub> oxidation rates and isotopic fractionation associated with oxidation

Wetland CH<sub>4</sub> fluxes are mainly regulated by aerobic microbial CH<sub>4</sub> oxidation (Segers, 1998; Whalen, 2005). Similar to previous measurements in another polygon center in the Lena River delta (Knoblauch et al., 2008), the surface horizon (0–5 cm) of the saturated polygon center holds a high potential methanotrophic activity with oxidation rates in the range of  $31.7 \pm 2.3 \text{ nmol h}^{-1} \text{ g dw}^{-1}$ , in spite of being prevalently water saturated. Measurements have shown dissolved O<sub>2</sub> concentrations of up to 100 % air saturation in this horizon even if the water table lies 10 cm above the soil surface. This saturation might be explained by this site’s high average



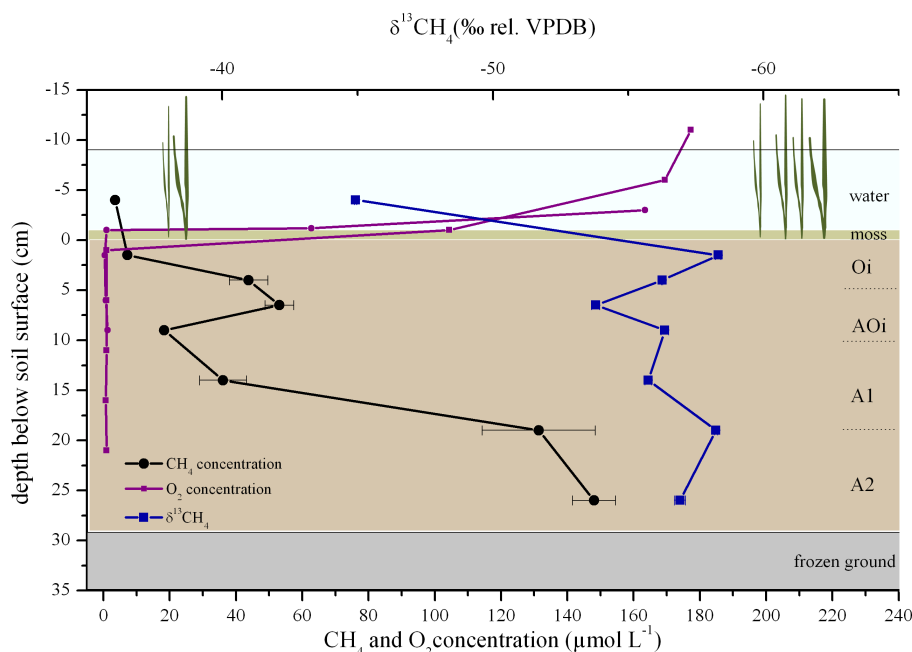


**Fig. 2.** Depth profiles of CH<sub>4</sub> concentration (black line, circles) and  $\delta^{13}\text{C}$  (blue line, squares) of saturated polygon center A on 19 July 2009 and depth profiles of O<sub>2</sub> concentration of the same polygon center on 8 July 2009 (purple line, squares) and 24 July 2009 (purple line, circles). Error bars represent the standard deviations of the means of two analytical replicates.

density 25 % of *Carex aquatilis*, a vascular plant with an internal gas-space ventilation system (aerenchyma) able to draw O<sub>2</sub> from the atmosphere to roots and rhizomes in the anoxic zone (Kutzbach et al., 2004), making it available for methane-oxidizing bacteria (Laanbroek, 2010).

In comparison, in the polygonal pond the highest potential oxidation rates are not found in the soil, but in the submerged brown moss layer ( $201 \pm 41 \text{ nmol h}^{-1} \text{ g dw}^{-1}$ ; Liebner et al., 2011). In contrast to the saturated polygon center, the average density of *Carex aquatilis* is much lower (6 %). Thus, the density of aerenchymatous sedges is likely to be a key factor for CH<sub>4</sub> oxidation rates in upper soil horizons of polygon centers under in situ conditions. The high potential methanotrophic activity of the thick, submerged brown moss layer of *Scorpidium scorpioides* in the polygonal pond has been explained with a mutualistic symbiosis of the moss with methanotrophic bacteria (Liebner et al., 2011).

With  $1.031 \pm 0.001$  the mean value of  $\alpha_{\text{ox}}$  of the top horizon of the polygon center A (Oi) is as high as values of landfill cover soils also determined at 4 °C (Chanton et al., 1999), where CH<sub>4</sub> oxidation rates are several orders higher in magnitude (Scheutz et al., 2009). While Teh et al. (2006) found  $\alpha_{\text{ox}}$  to be inversely proportional to the CH<sub>4</sub> oxidation rate ( $r^2 = 0.86$ ,  $p < 0.001$ ,  $n = 9$ ) in tropical rain forest soils with maximum oxidation rates between 8.2 and  $11.3 \text{ nmol h}^{-1} \text{ g dw}^{-1}$ , Pearson's regression analyses found a positive correlation of oxidation rates with  $\alpha_{\text{ox}}$  ( $r = 0.6$ ;  $p < 0.01$ ,  $n = 18$ ) across the two polygon centers and their

horizons. Moreover,  $\alpha_{\text{ox}}$  differed significantly between the polygon centers (mean  $\alpha_{\text{ox}} = 1.017 \pm 0.009$ ). Thus, the different sites probably host different methanotrophic communities with different  $\alpha_{\text{ox}}$ . Methanotrophs are generally divided into the three main groups type I, type II and type X, based on phylogeny and formaldehyde assimilation pathways, internal membrane arrangement and other biochemical characteristics (Kamal and Varma, 2008).

Moreover, isotopic fractionation associated with methanotrophic activity presumably occurs in the submerged brown moss layer of *Scorpidium scorpioides* in the polygonal pond as it has shown high oxidation rates in previous studies. Hence, when these mosses are abundant, their fractionation effect should be considered in addition to soil fractionation processes.

#### 4.2 Analysis of soil gas diffusivity and isotopic fractionation associated with diffusion

Since CH<sub>4</sub> diffusion alters the isotopic signature of the remaining gas phase, isotopic fractionation associated with diffusion needs to be taken into account in CH<sub>4</sub> efficiency calculations (Mahieu et al., 2008). Factors determining the soil gas diffusivity comprise air-filled porosity, the interconnectivity of the pore system and tortuosity. Results showed that diffusion occurred mainly through macropores. The exponential relationship between air-filled porosity and the diffusion coefficient is related to an increasing interconnectivity of pores with an increasing share of air-filled pores. The latter

effect has been observed in the same magnitude for mineral soils with lower air-filled porosities (Gebert et al. (2011),  $D_{\text{eff}} = 1.319 \times 10^{-7} \times e^{(\Phi \alpha / 0.116)} - 1.477 \times 10^{-7}$ ), but is less pronounced at higher porosities in comparison to mineral soils where the effects of tortuosity play a larger role. Soils with a larger air-filled porosity warrant higher diffusive gas supply of both O<sub>2</sub> into the uppermost soil horizon and CH<sub>4</sub> escaping from lower horizons.

This finding is in line with the low diffusion coefficients of the lowest horizon of the unsaturated polygon center (Table 3), which is characterized by higher bulk density and less air-filled porosity (Table 1). The higher potential diffusion rates at field capacity in the polygonal pond compared to the saturated polygon center might derive from the polygonal pond's higher mineral content creating a lower tortuosity.

Furthermore, the soil-water content strongly controls the diffusivity through determining the pore space available for gas phase transport and thus the fractionation by diffusion. Under water-saturated conditions almost no isotopic fractionation occurred ( $\alpha_{\text{diff}} = 1.001 \pm 0.000$ ). Under unsaturated conditions the isotopic fractionation by diffusion ranged between the theoretical maximum value in air  $\alpha_{\text{diff}} = 1.0195$  and the low isotopic fractionation during air–water gas transfer of  $\alpha_{\text{diff}} = 1.0008$  (Knox et al., 1992). The mean  $\alpha_{\text{diff}} = 1.013 \pm 0.003$  of the study sites at field capacity is lower than the maximum value of  $\alpha_{\text{diff}} = 1.0178 \pm 0.001$  assumed for sandy landfill cover soils (De Visscher et al., 2004), which is slightly less than the theoretical value of  $\alpha_{\text{diff}} = 1.0195$  in air. The fractionation factor determined by De Visscher et al. (2004) used glass beads, which presumably feature both a lower tortuosity and a higher pore interconnectedness than the peaty tundra soils. The higher diffusion coefficient in the porous medium ( $5.54 \times 10^{-6} \text{ m}^2 \text{ s}^{-1}$ ) could facilitate isotopic fractionation by diffusion. Measurements in this study showed no correlation between diffusion coefficients and  $\alpha_{\text{diff}}$ , but might show a different relationship with higher concentration gradients as found in landfill habitats where CH<sub>4</sub> concentrations up to 60 % are found at the bottom of cover soils (Cabral et al., 2010).

### 4.3 CH<sub>4</sub> oxidation efficiency calculations

The observed decrease in CH<sub>4</sub> concentration between the lower and the upper horizons of the saturated polygon center A cannot be explained by oxidation since no oxygen was available in these depths. Anaerobic oxidation of methane (AOM) was not considered since it is coupled to the reduction of electron acceptors such as sulfate, ferric iron, nitrate and nitrite (Blazewicz, 2012), and concentrations of these electron acceptors are too low in the organic-rich soils studied (Fiedler, 2004). In addition, AOM would cause a change in isotopic signatures, which was not detected here. Thus, the decrease in CH<sub>4</sub> concentration must originate from the different transport mechanisms (diffusive, advective or ebullitive with  $\alpha_{\text{trans}} = 1$ ). Moreover, the increase of CH<sub>4</sub> concentration

and lower  $\delta^{13}\text{C}_{\text{CH}_4}$  values between 6.5 and 1.5 cm imply further CH<sub>4</sub> production in a horizon where fresh organic material is available for microbial degradation. In this horizon CH<sub>4</sub> production and oxidation occur in close proximity.

Calculations indicated a CH<sub>4</sub> oxidation efficiency of up to 50 % in the first 1.5 cm of the saturated polygon center where oxygen is present. The highest methanotrophic activity expectedly occurs at the anaerobic–aerobic interface since the ratio of CH<sub>4</sub> to O<sub>2</sub> is optimal here (Dedysh, 2002). An oxidation efficiency of this magnitude seems reasonable and has been described before; e.g., peat cores from a fresh water marsh reached up to 32 % oxidation efficiency under water-saturated conditions (Roslev and King, 1996).

Wetlands inhabited by vascular plants show plant-mediated CH<sub>4</sub> transport as the predominant transport mechanism (Van Der Nat and Middelburg, 1998), which may account for up to two-thirds of the total flux in a water-saturated polygon center of the Siberian tundra (Kutzbach et al., 2004). The site used for the current study is characterized by an average density of *Carex aquatilis* of 25 %. The downward transport of O<sub>2</sub> of these plants is accompanied by an upward diffusion of CH<sub>4</sub> from the rhizosphere along the concentration gradient (Lai, 2009). This passive transport mechanism is accompanied by isotopic fractionation resulting in the emission of lighter CH<sub>4</sub> (Chanton and Whiting, 1996; Chasar et al., 1999). However, plant-mediated transport does not affect the CH<sub>4</sub> efficiency calculations as the CH<sub>4</sub> bypasses the aerobic layer and is therefore not available for oxidation.

Fractionation associated with diffusion can obscure calculations of total CH<sub>4</sub> production and oxidation. Since the effects of diffusion and oxidation on the isotopic signature of the remaining gas phase are of opposite direction, neglecting diffusive fractionation by setting  $\alpha_{\text{trans}}$  to 1 causes an underestimation of CH<sub>4</sub> oxidation; a lighter isotopic signature is observed that could misleadingly be interpreted as less oxidation efficiency. Therefore, the isotopic fractionation factor of transport is subtracted from the fractionation of oxidation in the CH<sub>4</sub> efficiency calculation. As a result, the calculated efficiency increases since the shift in  $\delta^{13}\text{C}$  values is caused by a smaller difference between  $\alpha_{\text{ox}}$  and  $\alpha_{\text{trans}}$ . However, results show that isotope fractionation by diffusion only plays a substantial role under unsaturated conditions. Thus, under water-saturated conditions  $\alpha_{\text{trans}}$  can be assumed to be 1. For the presented study sites of the polygonal tundra in the Siberian Lena River delta it seems plausible to use the mean  $\alpha_{\text{diff}} = 1.013$  under unsaturated conditions for CH<sub>4</sub> oxidation efficiency calculations when diffusion is the predominant transport mechanism since  $\alpha_{\text{diff}}$  did not differ significantly between sites. On the contrary, isotopic fractionation factors associated with oxidation differ strongly between sites and need to be determined for each oxic horizon of interest. The isotopic fractionation factors presented in the current study might be higher than under in situ conditions since they were determined in laboratory experiments applying high initial CH<sub>4</sub> concentrations (Templeton et al., 2006).

As previously mentioned by Nihous (2010), the calculated oxidation efficiency is only as reliable as the knowledge of the isotopic fractionation factors since slight variations in the adopted  $\alpha_{\text{ox}}$  and  $\alpha_{\text{trans}}$  change the outcome strongly. Especially under unsaturated conditions, the predominant transport mechanism has to be considered to obtain trustworthy oxidation efficiency values. Here, supplemental CH<sub>4</sub> emission measurements might help.

Including temperature-dependent corrections for the isotopic fractionation factors into the oxidation efficiency calculations results in higher oxidation efficiencies. Tyler et al. (1994) showed that the correlation between temperature and isotopic fractionation factor decreased with soil depth ranging between  $4.3\text{--}5.0 \times 10^{-4} \text{ } ^\circ\text{C}^{-1}$ . Further, Knoblauch et al. (2008) found with SI probing of microbial PLFAs that the community active in situ is dominated by type I methanotrophs and that rising temperatures increase the importance of type II in soils of the same area. Type II bacteria show a lower CH<sub>4</sub> oxidation activity and a lower  $\alpha_{\text{ox}}$  than type I (Zyakun and Zakharchenko, 1998). Differences in the carbon isotopic fractionation are due to the type of methane monooxygenase (MMO) expressed by the cells, the mechanism for assimilation of cell carbon and the type of cellular physiology (Jahnke et al., 1999). Each process of the first CH<sub>4</sub> oxidation step (adsorption and desorption from the cell wall and conversion to methanol) may proceed at a specific rate with a specific isotopic fractionation (Nihous, 2010). Thus, it is assumed that microbial communities of different ecosystems react unequally to temperature, and universal applications of correction factors seem problematic. Nonetheless, it is likely that  $\alpha_{\text{ox}}$  is directly influenced by soil temperature, and neglecting it might underestimate the CH<sub>4</sub> oxidation efficiency.

The presented study shows that isotope fractionation by diffusion could play an important role in wetland soils under unsaturated conditions resulting in higher calculated CH<sub>4</sub> oxidation efficiencies. However, these calculations have been conducted with  $\delta^{13}\text{C}$  profiles of water-saturated conditions. Thus, future measurements and CH<sub>4</sub> oxidation efficiency calculations need to be conducted for different water level conditions of the studied sites as they drive the strength of oxidation processes.

## 5 Conclusions

The isotopic fractionation factors presented here enable the calculation of the potential CH<sub>4</sub> oxidation efficiency in arctic wetland soils. To determine CH<sub>4</sub> oxidation efficiency, the isotopic fractionation factors associated with oxidation need to be determined for the oxic horizons of the site of interest since they strongly differ from site to site and horizon to horizon. Furthermore, the contribution of diffusion to other simultaneously occurring transport mechanisms has to be estimated by means of the interpretation of unsaturated/water-

saturated conditions and both the CH<sub>4</sub> concentration and SI soil profiles. A mean value of  $\alpha_{\text{diff}} = 1.013$  may be applied for the investigated polygonal tundra sites under unsaturated conditions, while under water saturation  $\alpha_{\text{diff}} = 1.001$  can be used. The experimental setup to determine the potential CH<sub>4</sub> oxidation efficiency at 4 °C gives conservative estimates. If feasible, isotopic fractionation factors should be determined at temperatures occurring in situ. To deepen the understanding of CH<sub>4</sub> oxidation efficiencies of northern wetland soils, it is essential to study soils of different hydrological regimes. These calculations could then provide the basis for an improved estimation of current CH<sub>4</sub> sources and sinks and their potential strength in response to environmental change and global warming, especially in permafrost-affected soils, which bear the potential to cause a positive feedback to climate change.

*Acknowledgements.* The authors would like to thank the members of the joint Russian–German expeditions LENA 2009 and 2010 and the staff of the Alfred Wegener Institute, Research Unit Potsdam, for logistical, technical and administrative support. Special thanks go to Susanne Liebner for the O<sub>2</sub> profile measurements and to Svetlana Evgrafova for additional pore-water sampling in 2010. Birgit Schwinge, Volker Kleinschmidt and Stephanie Langer from the Institute of Soil Science are acknowledged for their help with laboratory analyses and Benjamin Runkle for editing the English. This project is funded by the German Science Foundation through the Cluster of Excellence Integrated Climate System Analysis and Prediction (CliSAP), KlimaCampus Hamburg.

Edited by: P. Overduin

## References

- Åkerman, H. J. and Johansson, M.: Thawing permafrost and thicker active layers in sub-arctic Sweden, *Permafrost Periglac.*, 19, 279–292, 2008.
- Anisimov, O. A.: Potential feedback of thawing permafrost to the global climate system through methane emission, *Environ. Res. Lett.*, 2, 1–7, doi:10.1088/1748-9326/2/4/045016, 2007.
- Barker, J. F. and Fritz, P.: Carbon isotope fractionation during microbial methane oxidation, *Nature*, 293, 289–291, 1981.
- Bergamaschi, P., Lubina, C., Königstedt, R., Fischer, H., Veltkamp, A. C., and Zwaagstra, O.: Stable isotopic signatures ( $\delta\text{C-13}$ ,  $\delta\text{D}$ ) of methane from European landfill sites, *J. Geophys. Res.-Atmos.*, 103, 8251–8265, 1998.
- Blazewicz, S. J., Petersen, D. G., Waldrop, M. P., and Firestone, M. K.: Anaerobic oxidation of methane in tropical and boreal soils: Ecological significance in terrestrial methane cycling, *J. Geophys. Res.-Biogeosci.*, 117, G02033, blackboxPlease provide doi link., 2012.

- Boike, J., Wille, C., and Abnizova, A.: Climatology and summer energy and water balance of polygonal tundra in the Lena River Delta, Siberia, *J. Geophys. Res.-Biogeo.*, 113, 1–15, G03025, doi:10.1029/2007JG000540, 2008.
- Brand, W. A.: PreCon: A Fully Automated Interface for the Pre-Gc Concentration of Trace Gases on Air for Isotopic Analysis, *Isot. Environ. Healt. S.*, 31, 277–284, 1995.
- Braun-Blanquet, J.: *Pflanzensoziologie*, Springer, Wien, 1964.
- Cabral, A. R., Capanema, M. A., Gebert, J., Moreira, J. F., and Jugnia, L. B.: Quantifying Microbial Methane Oxidation Efficiencies in Two Experimental Landfill Biocovers Using Stable Isotopes, *Water Air Soil Poll.*, 209, 157–172, doi:10.1007/s11270-009-0188-4, 2010.
- Chanton, J. P.: The effect of gas transport on the isotope signature of methane in wetlands, *Org. Geochem.*, 36, 753–768, doi:10.1016/j.orggeochem.2004.10.007, 2005.
- Chanton, J. P. and Whiting, G. J.: Methane stable isotopic distributions as indicators of gas transport mechanisms in emergent aquatic plants, *Aquat. Bot.*, 54, 227–236, 1996.
- Chanton, J. P., Rutkowski, C. M., and Mosher, B.: Quantifying Methane Oxidation from Landfills Using Stable Isotope Analysis of Downwind Plumes, *Envir. Sci. Tech.*, 33, 3755–3760, 1999.
- Chanton, J. P., Glaser, P. H., Chasar, L. S., Burdige, D. J., Hines, M. E., Siegel, D. I., Tremblay, L. B., and Cooper, W. T.: Radiocarbon evidence for the importance of surface vegetation on fermentation and methanogenesis in contrasting types of boreal peatlands, *Global Biogeochem. Cy.*, 22, GB4022, doi:10.1029/2008gb003274, 2008a.
- Chanton, J. P., Powelson, D. K., Abichou, T., Fields, D., and Green, R.: Effect of Temperature and Oxidation Rate on Carbon-isotope Fractionation during Methane Oxidation by Landfill Cover Materials, *Envir. Sci. Tech.*, 42, 7818–7823, doi:10.1021/es801221y, 2008b.
- Chasar, L. S., Chanton, J. P., Glaser, P. H., and Siegel, D. I.: Methane concentration and stable isotope distribution as evidence of rhizospheric processes: Comparison of a fen and bog in the Glacial Lake Agassiz Peatland complex, XVIth International Botanical Congress, St Louis, Missouri, ISI:000089309600023, 655–663, 1999.
- Coleman, D. D., Risatti, J. B., and Schoell, M.: Fractionation of carbon and hydrogen isotopes by methane-oxidizing bacteria, *Geochim. Cosmochim. Ac.*, 45, 1033–1037, 1981.
- Coward, H. F. and Georgeson, E. H. M.: 226, The diffusion coefficient of methane and air, *J. Chem. Soc. (Resumed)*, 1085–1087, 226, doi:10.1039/JR9370001085, 1937.
- Curry, C. L.: The consumption of atmospheric methane by soil in a simulated future climate, *Biogeosciences*, 6, 2355–2367, doi:10.5194/bg-6-2355-2009, 2009.
- De Visscher, A., Thomas, D., Boeckx, P., and Van Cleemput, O.: Methane Oxidation in Simulated Landfill Cover Soil Environments, *Envir. Sci. Tech.*, 33, 1854–1859, doi:10.1021/es9900961, 1999.
- De Visscher, A., De Pourcq, I., and Chanton, J.: Isotope fractionation effects by diffusion and methane oxidation in landfill cover soils, *J. Geophys. Res.-Atmos.*, 109, 1–8, doi:10.1029/2004jd004857, 2004.
- Dedush, S. N.: Methanotrophic Bacteria of Acidic Sphagnum Peat Bogs, *Microbiology*, 71, 638–650, doi:10.1023/a:1021467520274, 2002.
- Dlugokencky, E. J., Bruhwiler, L., White, J. W. C., Emmons, L. K., Novelli, P. C., Montzka, S. A., Masarie, K. A., Lang, P. M., Crotwell, A. M., Miller, J. B., and Gatti, L. V.: Observational constraints on recent increases in the atmospheric CH<sub>4</sub> burden, *Geophys. Res. Lett.*, 36, 1–5, L18803, doi:10.1029/2009gl0139780, 2009.
- Dueñas, C., Fernández, M. C., Carretero, J., Pérez, M., and Liger, E.: Consumption of methane by soils, *Environ. Monit. Assess.*, 31, 125–130, doi:10.1007/bf00547187, 1994.
- Fiedler, S., Wagner, D., Kutzbach, L., and Pfeiffer, E. M.: Element redistribution along hydraulic and redox gradients of low-centered polygons, Lena Delta, northern Siberia, *Soil Science Society of America Journal*, 68, 1002–1011, 2004.
- Forster, P., Ramaswamy, V., Artaxo, P., Bernsten, T., Betts, R., Fahey, D. W., Haywood, J., Lean, J., Lowe, D. C., Myhre, G., Nganga, J., Prinn, R., Raga, G., Schulz, M., and Van Dorland, R.: Changes in Atmospheric Constituents and in Radiative Forcing, in: *Climate Change 2007: The Physical Science Basis, Contribution of Working Group I to the Fourth Assessment Report of the Intergovernmental Panel on Climate Change*, edited by: Solomon, S., Qin, D., Manning, M., Chen, Z., Marquis, M., Averyt, K. B., Tignor, M., and Miller, H. L., Cambridge, UK and NY, NY, USA, 2007.
- French, H. M.: *The Periglacial Environment*, 2nd Edn., Longman Singapore, 376 pp., 1996.
- Gebert, J., Groengroeft, A., and Miehlich, G.: Kinetics of microbial landfill methane oxidation in biofilters, *Waste Manage.*, 23, 609–619, 2003.
- Gebert, J., Groengroeft, A., and Pfeiffer, E.-M.: Relevance of soil physical properties for the microbial oxidation of methane in landfill covers, *Soil Biol. Biochem.*, 43, 1759–1767, 2011.
- Gomez, K., Gonzalez-Gil, G., Schroth, M. H., and Zeyer, J.: Transport of methane and noble gases during gas push-pull tests in variably saturated porous media, *Envir. Sci. Tech.*, 42, 2515–2521, doi:10.1021/es072036y, 2008.
- Happell, J. D., Chanton, J. P., and Showers, W. S.: The influence of methane oxidation on the stable isotopic composition of methane emitted from Florida swamp forests, *Geochim. Cosmochim. Ac.*, 58, 4377–4388, 1994.
- Huber-Humer, M., Roder, S., and Lechner, P.: Approaches to assess biocover performance on landfills, *Waste Manage.*, 29, 2092–2104, doi:10.1016/j.wasman.2009.02.001, 2009.
- Jahnke, L. L., Summons, R. E., Hope, J. M., and Des Marais, D. J.: Carbon isotopic fractionation in lipids from methanotrophic bacteria II: the effects of physiology and environmental parameters on the biosynthesis and isotopic signatures of biomarkers, *Geochim. Cosmochim. Ac.*, 63, 79–93, 1999.
- Joabsson, A., Christensen, T. R., and Wallen, B.: Vascular plant controls on methane emissions from northern peatforming wetlands, *Trends Ecol. Evol.*, 14, 385–388, 1999.
- Kamal, S. and Varma, A.: Peatland Microbiology, in: *Microbiology of Extreme Soils*, edited by: Dion, P., and Nautiyal, C. S., Soil Biology, Springer Berlin Heidelberg, 177–203, 2008.
- Keppler, F., Hamilton, J. T. G., Brass, M., and Rockmann, T.: Methane emissions from terrestrial plants under aerobic conditions, *Nature*, 439, 187–191, doi:10.1038/nature04420, 2006.
- Knoblauch, C., Zimmermann, U., Blumenberg, M., Michaelis, W., and Pfeiffer, E. M.: Methane turnover and temperature response of methane-oxidizing bacteria in permafrost-affected

- soils of northeast Siberia, *Soil Biol. Biochem.*, 40, 3004–3013, doi:10.1016/j.soilbio.2008.08.020, 2008.
- Knox, M., Quay, P. D., and Wilbur, D.: Kinetic Isotopic Fractionation During Air-Water Gas Transfer of O<sub>2</sub>, N<sub>2</sub>, CH<sub>4</sub>, and H<sub>2</sub>, *J. Geophys. Res.-Oceans*, 97, 20335–20343, doi:10.1029/92jc00949, 1992.
- Kutzbach, L., Wagner, D., and Pfeiffer, E. M.: Effect of microrelief and vegetation on methane emission from wet polygonal tundra, Lena Delta, Northern Siberia, *Biogeochemistry*, 69, 341–362, 2004.
- Laanbroek, H. J.: Methane emission from natural wetlands: interplay between emergent macrophytes and soil microbial processes, A mini-review, *Ann. Bot.*, 105, 141–153, doi:10.1093/aob/mcp201, 2010.
- Lai, D. Y. F.: Methane Dynamics in Northern Peatlands: A Review, *Pedosphere*, 19, 409–421, 2009.
- Liebner, S., Zeyer, J., Wagner, D., Schubert, C., Pfeiffer, E.-M., and Knoblauch, C.: Methane oxidation associated with submerged brown mosses reduces methane emissions from Siberian polygonal tundra, *J. Ecol.*, 99, 914–922, doi:10.1111/j.1365-2745.2011.01823.x, 2011.
- Liptay, K., Chanton, J., Czepiel, P., and Mosher, B.: Use of stable isotopes to determine methane oxidation in landfill cover soils, *J. Geophys. Res.-Atmos.*, 103, 8243–8250, 1998.
- Mahieu, K., De Visscher, A., Vanrolleghem, P. A., and Van Cleemput, O.: Modelling of stable isotope fractionation by methane oxidation and diffusion in landfill cover soils, *Waste Management*, 28, 1535–1542, doi:10.1016/j.wasman.2007.06.003, 2008.
- McKinney, C. R., McCrea, J. M., Epstein, S., Allen, H. A., and Urey, H. C.: Improvements in mass spectrometers for the measurement of small differences in isotope abundance ratios, *Rev. Sci. Instrum.*, 21, 724–730, doi:10.1063/1.1745698, 1950.
- Monson, K. D. and Hayes, J. M.: Biosynthetic control of the natural abundance of carbon 13 at specific positions within fatty acids in *Escherichia coli*, Evidence regarding the coupling of fatty acid and phospholipid synthesis, *J. Biol. Chem.*, 255, 1435–1441, 1980.
- Nauer, P. A. and Schroth, M. H.: In Situ Quantification of Atmospheric Methane Oxidation in Near-Surface Soils, *Vadose Zone J.*, 9, 1052–1062, doi:10.2136/vzj2009.0192, 2010.
- Nihous, G. C.: Notes on the temperature dependence of carbon isotope fractionation by aerobic CH<sub>4</sub>-oxidising bacteria, *Isot. Environ. Healt. S.*, 46, 133–140, doi:10.1080/10256016.2010.488724, 2010.
- Nozhevnikova, A., Glagolev, M., Nekrasova, V., Einola, J., Sormunen, K., and Rintala, J.: The analysis of methods for measurement of methane oxidation in landfills, *Water Sci. Technol.*, 48, 45–52, 2003.
- Powelson, D. K., Charlton, J. P., and Abichou, T.: Methane oxidation in biofilters measured by mass-balance and stable isotope methods, *Envir. Sci. Technol.*, 41, 620–625, doi:10.1021/es061656g, 2007.
- Rayleigh, J. W. S.: Theoretical Considerations respecting the Separation of Gases by Diffusion and Similar Processes, *Philos. Mag.*, 42, 493–498, 1896.
- Reeburgh, W. S., Hirsch, A. I., Sansone, F. J., Popp, B. N., and Rust, T. M.: Carbon kinetic isotope effect accompanying microbial oxidation of methane in boreal forest soils, *Geochim. Cosmochim. Ac.*, 61, 4761–4767, 1997.
- Richards, L. A. and Fireman, M.: Pressure plate apparatus for measuring moisture sorption and transmission by soil, *Soil Sci.*, 56, 395–404, 1943.
- Rolston, D. E.: Gas diffusivity, in: *Methods of Soil Analysis, Part 1. Physical and Mineralogical Methods – Agronomy Monograph No. 9, 2nd Edn.*, American Society of Agronomy – Soil Sci. Soc. America, 1986.
- Roslev, P. and King, G. M.: Regulation of methane oxidation in a freshwater wetland by water table changes and anoxia, *Fems Microbiol. Ecol.*, 19, 105–115, 1996.
- Scheutz, C., Kjeldsen, P., Bogner, J. E., De Visscher, A., Gebert, J., Hilger, H. A., Huber-Humer, M., and Spokas, K.: Microbial methane oxidation processes and technologies for mitigation of landfill gas emissions, *Waste Manage. Res.*, 27, 409–455, doi:10.1177/0734242x09339325, 2009.
- Schneider, J., Grosse, G., and Wagner, D.: Land cover classification of tundra environments in the Arctic Lena Delta based on Landsat 7 ETM+ data and its application for upscaling of methane emissions, *Remote Sens. Environ.*, 113, 380–391, doi:10.1016/j.rse.2008.10.013, 2009.
- Schuur, E. A. G., Vogel, J. G., Crummer, K. G., Lee, H., Sickman, J. O., and Osterkamp, T. E.: The effect of permafrost thaw on old carbon release and net carbon exchange from tundra, *Nature*, 459, 556–559, 2009.
- Segers, R.: Methane production and methane consumption: a review of processes underlying wetland methane fluxes, *Biogeochemistry*, 41, 23–51, 1998.
- Seibt, A., Hoth, P., and Naumann, D.: Gas solubility in formation waters of the North German Basin – implications for geothermal energy recovery, in: *Proceedings World Geothermal Congress 2000, Kyushu-Tohoku, Japan, 1713–1718*, 2000.
- Streese-Kleeberg, J., Rachor, I., Gebert, J., and Stegmann, R.: Use of gas push-pull tests for the measurement of methane oxidation in different landfill cover soils, *Waste Manage.*, 31, 995–1001, 2011.
- Sundh, I., Mikkilä, C., Nilsson, M., and Svensson, B. H.: Potential aerobic methane oxidation in a Sphagnum-dominated peatland, Controlling factors and relation to methane emission, *Soil Biol. Biochem.*, 27, 829–837, 1995.
- Tagesson, T., Mölder, M., Mastepanov, M., Sigsgaard, C., Tamstorf, M. P., Lund, M., Falk, J. M., Lindroth, A., Christensen, T. R., and Ström, L.: Land-atmosphere exchange of methane from soil thawing to soil freezing in a high-Arctic wet tundra ecosystem, *Glob. Change Biol.*, 18, 1928–1940, doi:10.1111/j.1365-2486.2012.02647.x, 2012.
- Tarnocai, C., Canadell, J. G., Schuur, E. A. G., Kuhry, P., Mazhitova, G., and Zimov, S.: Soil organic carbon pools in the northern circumpolar permafrost region, *Glob. Biogeochem. Cy.*, 23, doi:10.1029/2008gb003327, 2009.
- Teh, Y. A., Silver, W. L., Conrad, M. E., Borglin, S. E., and Carlson, C. M.: Carbon isotope fractionation by methane-oxidizing bacteria in tropical rain forest soils, *J. Geophys. Res.*, 111, G02001, doi:10.1029/2005jg000053, 2006.
- Templeton, A. S., Chu, K. H., Alvarez-Cohen, L., and Conrad, M. E.: Variable carbon isotope fractionation expressed by aerobic CH<sub>4</sub>-oxidizing bacteria, *Geochim. Cosmochim. Ac.*, 70, 1739–1752, doi:10.1016/j.gca.2005.12.002, 2006.
- Tyler, S. C., Crill, P. M., and Brailsford, G. W.: <sup>13</sup>C/<sup>12</sup>C Fractionation of methane during oxidation in a temperate forested soil,

- Geochim. Cosmochim. Ac., 58, 1625–1633, 1994.
- Urmann, K., Gonzalez-Gil, G., Schroth, M. H., and Zeyer, J.: Quantification of microbial methane oxidation in an alpine peat bog, *Vadose Zone J.*, 6, 705–712, doi:10.2136/vzj2006.0185, 2007.
- USDA: Keys to Soil Taxonomy, 11th Edn., edited by: Service, N. R. C., United States Department of Agriculture, Soil Survey Staff, 2010.
- Van Der Nat, F.-J. W. A., and Middelburg, J. J.: Effects of two common macrophytes on methane dynamics in freshwater sediments, *Biogeochemistry*, 43, 79–104, doi:10.1023/a:1006076527187, 1998.
- Walter, K. M., Smith, L. C., and Chapin, F. S.: Methane bubbling from northern lakes: present and future contributions to the global methane budget, *Philos. T. R. Soc.*, 365, 1657–1676, doi:10.1098/rsta.2007.2036, 2007.
- Wang, J. S., Logan, J. A., McElroy, M. B., Duncan, B. N., Megretskaia, I. A., and Yantosca, R. M.: A 3-D model analysis of the slowdown and interannual variability in the methane growth rate from 1988 to 1997, *Global Biogeochem. Cy.*, 18, 1–30, GB3011, doi:10.1029/2003gb002180, 2004.
- Whalen, S. C.: Biogeochemistry of methane exchange between natural wetlands and the atmosphere, *Environ. Eng. Sci.*, 22, 73–94, 2005.
- Wille, C., Kutzbach, L., Sachs, T., Wagner, D., and Pfeiffer, E. M.: Methane emission from Siberian arctic polygonal tundra: eddy covariance measurements and modeling, *Global Change Biol.*, 14, 1395–1408, doi:10.1111/j.1365-2486.2008.01586.x, 2008.
- WRB, I. W. G.: World reference base for soil resources 2006, Food and Agriculture Organization of the United Nations, Rome, 2006.
- Yamamoto, S., Alcauskas, J. B., and Crozier, T. E.: Solubility of Methane in Distilled Water and Seawater, *J. Chem. Eng. Data*, 21, 78–80, doi:10.1021/je60068a029, 1976.
- Zubrzycki, S., Kutzbach, L., Grosse, G., Desyatkin, A., and Pfeiffer, E.-M.: Organic Carbon and Total Nitrogen Stocks in Soils of the Lena River Delta, *Biogeosciences*, accepted, 2013.
- Zyakun, A. M. and Zakharchenko, V. N.: Carbon isotope discrimination by methanotrophic bacteria: Practical use in biotechnological research (review), *Appl. Biochem. Microbiol.*, 34, 207–219, 1998.